I. Troch, F. Breitenecker, eds. ISBN 978-3-901608-35-3

WAVE PROPAGATION IN PERIODICALLY EXCITED FLUID TRANSMISSION LINES WITH A NONLINEAR COMPRESSIBILITY LAW

B. Manhartsgruber
Johannes Kepler University, Linz, Austria, Institute of Machine Design and Hydraulic Drives
Altenbergerstraße 69, 4040 Linz, Austria; bernhard.manhartsgruber@jku.at

Abstract. Pipelines filled with a weakly compressible fluid such as mineral oil or water play an important role in many fields of technology such as internal combustion engines or hydraulic drives. A number of interesting problems such as the prediction of pressure ripples for piston pumps or the simulation of fuel injections systems at a single operating point share the property of periodic boundary conditions. The phenomenon of wave propagation in transmission lines is well understood in the case of a weakly compressible fluid with a linear material law. For this type of problem, the periodic case can be treated with high computational efficiency by using transcendental transfer functions in the frequency domain. This paper aims at the computation of pressure and flow waves arising in liquid transmission lines with periodic pressure and/or flow boundary conditions and a nonlinear law of liquid compressibility. The nonlinearity is due to the presence of small gas bubbles in the liquid. This condition frequently occurs in the low pressure part of fluid power systems where dissolved air is released. An isothermal behaviour of the gas bubbles is assumed in this paper for computational simplicity. The validity of this assumption or more likely the need for a refined model with a detailed description of the gas behaviour will be the focus of experiments in the near future.

1 Introduction

Fluid transmission lines are abundant in many fields of science and technology beginning from ancient irrigation systems to modern distribution systems for many different fluids like potable water, crude oil or natural gas. The first applications of wave propagation theory to fluid transmission lines can be traced back to the second half of the nineteenth century with the influental work of Joukowsky on the waterhammer phenomenon in the St. Petersburg waterworks [5]. Similar phenomena occured with respect to sudden valve closure in the penstocks of hydropower plants [9]. The dynamic behaviour of oil and gas pipelines has been of major interest in the second half of the twentieth century. While these systems can reach lengths of several thousand kilometres, they share many properties with shorter systems operated at higher frequencies occuring in fluid power systems and especially in modern fuel injection and valve actuations systems for internal combustion engines. In steady-state operation, these systems feature a periodic excitation of the fluid transmission lines. In many cases, the pressure amplitudes are small enough to justify a linearization of the fluid's material law. Often, the models are used to optimize the transmission line geometry or the operating conditions in order to minimize pressure amplitudes. Here it makes sense to use a linearized model even if it is only a poor description of the reality for the starting point of the optimization. If the pressure ripples can successfully be minimized, the model is valid in the end. A frequency domain approach is widely used for this kind of problems because of the compact description of dissipative effects occuring in fluid filled transmission lines. The so called frequency-dependent friction is easily described in the frequency domain while a time domain approximation is difficult.

However, there are counterexamples where a linearized model can no longer be used. One possibility is to use three-dimensional CFD-codes in these cases [2]. However, the computational cost is very high and a systematic analysis of the solution behaviour of the nonlinear systems under periodic excitation including a bifurcation analysis is often impossible. The use of time integration methods designed for initial value problems in order to compute periodic solutions is especially cumbersome if the systems are weakly damped [6].

This paper focusses on the case of liquid transmission lines under low pressure conditions: Dissolved air is released and forms small bubbles which deteriorate the stiffness of the fluid which is now a mixture of the base liquid and the air bubbles. The process of air release is triggered by low pressure and agitation of the fluid. It is counterbalanced by a process of back-solution of gas into the liquid which takes place at high pressure and on a much longer time scale than the air release process. For the material law used in this paper, no dynamics of air release and solution is taken into account, the derivation in the next section simply assumes the presence of a certain share of gas bubbles in the fluid. The mass fraction of free gas bubbles vs. liquid therefore remains constant. However, the size of the gas bubbles and thus the mean density of the mixture is strongly influenced by the hydrostatic pressure.

The main motivation behind this paper is to develop a model that can be compared to experimental results in order to evaluate the assumptions made for the behaviour of the gas fraction. The model will probably need some amendments once experimental data is available.

2 A nonlinear transmission line model

2.1 The material model

As outlined in the introduction, throughout this paper the fluid in the transmission line is assumed to be a mixture of a carrier liquid with a certain amount of evenly distributed small gas bubbles. The material law is derived as a relation between pressure and mean density in a variable volume filled with the aforementioned mixture. An isothermal state equation for the gas phase

$$p_0 V_{0,gas} = p V_{gas}. \tag{1}$$

is assumed for the sake of simplicity. At the reference pressure level p_0, the volumetric ratio of gas vs. liquid is parameterized as

$$\alpha = \frac{V_{0,gas}}{V_{0,oil}}. \tag{2}$$

The liquid phase is assumed to obey the affine equation

$$\rho_{liq} = \rho_0 \left(1 + \frac{p - p_0}{E_{liq}}\right). \tag{3}$$

linking the hydrostatic pressure p with the density ρ_{liq} of the pure liquid without gas bubbles. The modulus of compressibility of the liquid phase is denoted by E_{liq}, whereas ρ_0 obviously is the liquid density at reference pressure. As already mentioned, the goal is to derive an expression for the mean mass density. Given the volumes V_{gas} and V_{liq} as well as the masses m_{gas} and m_{liq} of the two phases, this can be readily written in the form

$$\rho = \frac{m_{oil} + m_{gas}}{V_{oil} + V_{gas}}.$$

The masses are conserved throughout any state change of the system. For the liquid mass we find

$$m_{liq} = \rho_0 V_{0,liq},$$

whereas the mass of the gas fraction can be computed from the state equation of an ideal gas

$$m_{gas} = \frac{p_0 V_{0,gas}}{R_s T}.$$

The volume of the liquid fraction at a certain pressure is given by its initial volume and the density change due to eq. (3) whereas the volume of the gas fraction is given by eq. (1). Substitution of these results in the definition of the average density yields

$$\rho = \frac{\rho_0 V_{0,liq} + \frac{p_0 V_{0,gas}}{R_s T}}{\frac{V_{0,liq}}{1+\frac{p-p_0}{E_{oil}}} + V_{0,gas}\frac{p_0}{p}}.$$

This can be further simplified by use of the volumetric ratio α according to eq. (2):

$$\rho = \frac{\rho_0 + \frac{\alpha p_0}{R_s T}}{\frac{1}{1+\frac{p-p_0}{E_{oil}}} + \alpha\frac{p_0}{p}} \tag{4}$$

2.2 Conservation of mass and momentum

As outlined in the introduction, the pipe flow problem can be treated as a one-dimensional wave propagation problem with a dynamic friction model covering the effect of the radial velocity distribution. Thus the flow rate $Q(x,t)$ is used instead of the axial velocity in the following equations.

The conservation of mass along the transmission line simply reads

$$R^2\pi \frac{\partial}{\partial t}\rho(x,t) = -\frac{\partial}{\partial x}\left(\rho(x,t)\, Q(x,t)\right).$$

The momentum balance in axial direction requires

$$\frac{D}{Dt}\left(\rho\left(x,t\right)\frac{Q\left(x,t\right)}{R^2\pi}\right) = -\frac{\partial}{\partial x}p\left(x,t\right) - \rho\left(x,t\right)F\left(Q\left(x,t\right)\right)$$

where $F\left(Q\left(x,t\right)\right)$ denotes the deceleration due to viscous friction. In the stationary case, the pressure drop is given by the Hagen-Poiseuille law as

$$F\left(Q\left(x,t\right)\right) = \frac{8\nu}{R^4\pi}Q\left(x,t\right).$$

For the instationary yet laminar case, a frequency domain description is available in the form

$$F\left(Q\left(x,t\right)\right) = \frac{s}{R^2\pi}\left(\frac{J_0\left(\sqrt{-\frac{s}{\nu}}R\right)}{J_2\left(\sqrt{-\frac{s}{\nu}}R\right)} + 1\right)\hat{Q}\left(x,s\right)$$

where s denotes the Laplace variable. The derivation of this model can be found in [1, 4].

2.3 A scaled model

A proper scaling of the mathematical model is desirable for two reasons. Firstly, a dimensionless model usually contains a reduced set of parameters giving better insight into the parameter influence. Secondy, the scaling can be used to improve the numerical properties of the model.

In a first step, the independent variables x and t are replaced by dimensionless coordinates ξ and τ. The axial coordinate is re-scaled by the line length L, i. e.

$$\xi = \frac{x}{L}.$$

For the time scaling, the time-periodic nature of the problem suggests a scaling with the excitation frequency

$$\tau = \omega_{exc}t.$$

The time period of the periodic wave propagation problem is thus mapped onto the interval $0 \leq \tau \leq 2\pi$. The pressure is scaled by a characteristic pressure p_s, for instance a supply pressure value or a typical pressure excitation amplitude:

$$\psi\left(\xi,\tau\right) = \frac{p\left(x,t\right)}{p_s}$$

The flow rate scaling

$$q\left(\xi,\tau\right) = \frac{\sqrt{E\rho_0}}{p_s R^2\pi}Q\left(x,t\right)$$

is motivated by the Joukowsky relation. A unity step in the scaled pressure ψ will result in a unity step in the scaled flow rate q and vice versa. The material law (4) is scaled using the mass density ρ_0 of the fluid at the reference pressure p_0. This can be written as

$$\tilde{\rho} = \frac{\rho}{\rho_0} = \left(1 + \alpha\frac{p_0}{\rho_0 R_s T}\right)\frac{\psi + \frac{p_s}{E}\left(\psi^2 - \frac{p_0}{E}\psi\right)}{\psi + \alpha\frac{p_0}{E} + \alpha\frac{p_s p_0}{E^2}\left(\psi - \frac{p_0}{E}\right)}.$$

By defining the dimensionless parameters

$$\varepsilon = \frac{p_s}{E}, \quad \psi_0 = \frac{p_0}{p_s}, \quad \tilde{\rho}_\alpha = \frac{p_0}{\rho_0 R_s T}$$

the material law reads

$$\tilde{\rho} = \left(1 + \alpha\tilde{\rho}_\alpha\right)\frac{\left(1 - \varepsilon\psi_0\right)\psi + \varepsilon\psi^2}{\alpha\left(\psi_0 - \varepsilon\psi_0^2\right) + \left(1 + \alpha\varepsilon\psi_0\right)\psi}. \tag{5}$$

Using a scaled excitation frequency $\tilde{\omega}$ and the dissipation number D_n [3]

$$\tilde{\omega} = \omega_{exc}\frac{L}{\sqrt{\frac{E}{\rho_0}}} \qquad D_n = \frac{\nu L}{\sqrt{\frac{E}{\rho_0}}R^2},$$

the equation of continuity takes the dimensionless form

$$\tilde{\omega}\dot{\tilde{\rho}} = -\varepsilon\left(\tilde{\rho}'q + \tilde{\rho}q'\right). \tag{6}$$

The scaled momentum balance reads

$$\left(\tilde{\omega}\dot{\tilde{\rho}} + \varepsilon\left(\tilde{\rho}'q + \tilde{\rho}q'\right)\right)q + \tilde{\omega}\tilde{\rho}\dot{q} = -\psi' - 8D_n\tilde{\rho}f(q).$$

Obviously, this can be simplified by use of the continuity eq. (6) to

$$\tilde{\omega}\tilde{\rho}\dot{q} = -\psi' - 8D_n\tilde{\rho}f(q). \tag{7}$$

If only the stationary Hagen-Poiseuille friction is taken into account, the friction operator would simply be the identity $f(q) = q$. The frequency-dependent friction model as derived in [1] results in a dimensionless friction operator defined in the frequency domain by

$$\hat{f}(\hat{q}) = s\left(\frac{J_0\left(\sqrt{-\frac{\tilde{s}}{D_n}}\right)}{J_2\left(\sqrt{-\frac{\tilde{s}}{D_n}}\right)} + 1\right)\hat{q} \tag{8}$$

with $\tilde{s}$ denoting the Laplace variable in the dimensionless frequency.

3 Discretization in space

3.1 Reformulation of the equations

The three equations (5-7) in the independent variables τ and ξ define the evolution of the pressure ψ, flow-rate q and density ρ. As the material law (5) is an algebraic equation already explicit in the density ρ, it is substituted in the other two equations to reduce the number of unknowns. The resulting continuity equation can be written with a common denominator $\left(\alpha\left(\psi_0 - \varepsilon\psi_0^2\right) + (1 + \alpha\varepsilon\psi_0)\psi\right)^2$ obviously due to the denominator in the material law (5). From physical considerations, this denominator is strictly positive. Therefore, the whole equation can be multipied by the common denominator resulting in

$$\begin{aligned}
&\varepsilon\psi^2\left(\tilde{\omega}\dot{\psi} + q'\right) + \varepsilon^2\psi^2\left(\psi q' + q\psi'\right) + \alpha\psi_0\tilde{\omega}\dot{\psi} + \varepsilon\alpha\psi_0\left(\psi q' + q\psi' + 2\tilde{\omega}\psi\dot{\psi}\right) - \varepsilon^2\psi_0\psi^2 q' + \\
&\varepsilon^2\alpha\psi_0\psi\left(2\left(\psi q' + q\psi'\right) + \tilde{\omega}\psi\dot{\psi}\right) - 2\varepsilon\alpha\psi_0^2\tilde{\omega}\dot{\psi} + \varepsilon^3\alpha\psi_0\psi^2\left(\psi q' + q\psi'\right) - 2\varepsilon^2\alpha\psi_0^2\left(\psi q' + q\psi' + \tilde{\omega}\psi\dot{\psi}\right) + \\
&\varepsilon^2\alpha\psi_0^3\tilde{\omega}\dot{\psi} - 2\varepsilon^3\alpha\psi_0^2\psi\left(\psi q' + q\psi'\right) + \varepsilon^3\alpha\psi_0^3\left(\psi q' + q\psi'\right) = 0
\end{aligned} \tag{9}$$

where all terms have been sorted in ascending order with respect to their order in the parameters ε, α, and ψ_0. These three parameters are small compared to unity. Equation (10) lacks a zero order term regarding the small parameters. The lowest order term is a product of the liquid compressibility parameter ε, the squared dimensionless pressure ψ^2, and a bracket term which coincides with the continuity equation of the linearized problem. This motivates to divide the whole equation by the positive factor $\varepsilon\psi^2$ resulting in

$$\begin{aligned}
&\left(\tilde{\omega}\dot{\psi} + q'\right) + \varepsilon\left(\psi q' + q\psi'\right) + \frac{\alpha\psi_0}{\varepsilon}\tilde{\omega}\frac{\dot{\psi}}{\psi^2} + \alpha\psi_0\frac{\left(\psi q' + q\psi' + 2\tilde{\omega}\psi\dot{\psi}\right)}{\psi^2} - \varepsilon\psi_0 q' + \\
&\varepsilon\alpha\psi_0\left(2\left(q' + q\frac{\psi'}{\psi}\right) + \tilde{\omega}\dot{\psi}\right) - 2\alpha\psi_0^2\tilde{\omega}\frac{\dot{\psi}}{\psi^2} + \varepsilon^2\alpha\psi_0\left(\psi q' + q\psi'\right) - 2\varepsilon\alpha\psi_0^2\left(\frac{q'}{\psi} + \frac{q\psi'}{\psi^2} + \tilde{\omega}\frac{\dot{\psi}}{\psi}\right) + \\
&\varepsilon\alpha\psi_0^3\tilde{\omega}\frac{\dot{\psi}}{\psi^2} - 2\varepsilon^2\alpha\psi_0^2\left(q' + q\frac{\psi'}{\psi}\right) + \varepsilon^2\alpha\psi_0^3\left(\frac{q'}{\psi} + q\frac{\psi'}{\psi^2}\right) = 0
\end{aligned} \tag{10}$$

The continuity equation for the linear case – i. e. a liquid without gas bubbles under the assumption of a constant bulk modulus of compressibility – is the leading, zero order term. All other terms are perturbations of the linear case due to the nonlinearities arising from the presence of gas bubbles. This enables the embedding of the nonlinear problem in the linear one, which is the motivation for the rearrangement of the equations performed in this section.

The momentum balance eq. (7) is now treated in the same fashion. Omitting the common, strictly positive denominator $\alpha\left(\psi_0 - \varepsilon\psi_0^2\right) + (1 + \alpha\varepsilon\psi_0)\psi$ and sorting the terms in ε, α, ψ_0, and ρ_α, the momentum balance is

$$\psi\left(\tilde{\omega}\dot{q}+\psi'-f(q)\right)+\varepsilon\psi^2\left(\tilde{\omega}\dot{q}-f(q)\right)+\alpha\psi_0\psi'+\left(\alpha\rho_\alpha-\varepsilon\psi_0\right)\psi\left(\tilde{\omega}\dot{q}-f(q)\right)+$$
$$\varepsilon\alpha\psi_0\psi\psi'+\varepsilon\alpha\rho_\alpha\psi^2\left(\tilde{\omega}\dot{q}-f(q)\right)-\varepsilon\alpha\psi_0^2\psi'-\varepsilon\alpha\rho_\alpha\psi_0\psi\left(\tilde{\omega}\dot{q}-f(q)\right)=0$$

A division of the whole equation by the dimensionless pressure ψ results in

$$(1+\alpha\rho_\alpha)(1-\varepsilon\psi_0)\left(\tilde{\omega}\dot{q}-f(q)\right)+(1+\varepsilon\alpha\psi_0)\psi'+\varepsilon(1+\alpha\rho_\alpha)\psi\left(\tilde{\omega}\dot{q}-f(q)\right)+\alpha\psi_0(1-\varepsilon\psi_0)\frac{\psi'}{\psi}=0 \quad (11)$$

where the zero order term in the perturbation paramters ε, α, ψ_0, and ρ_α is the momentum balance for the linear case.

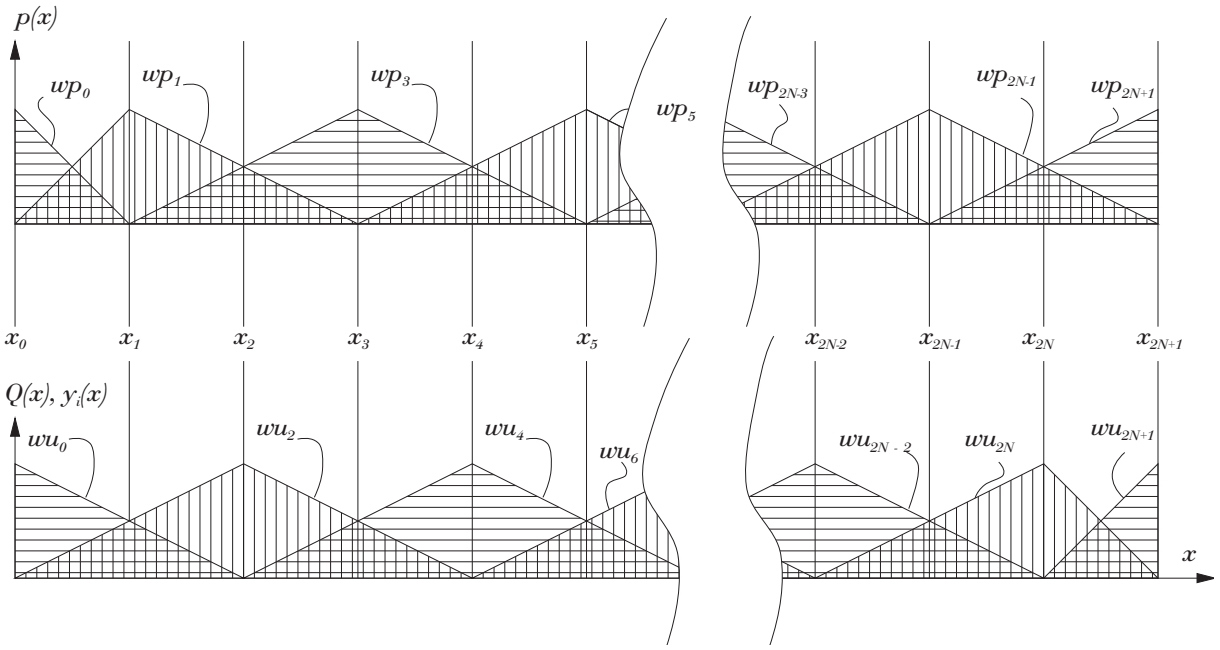

Figure 1: Interlacing grid for pressure and flow.

3.2 Interlacing grid for pressure and flow

An interlacing or staggered grid [7]for pressure and flow variables according to Fig. 1 with a number of $2N+2$ equally spaced grid points $x_i = L\frac{i}{2N+1}, i = 1,2,\ldots 2N+1$ has some advantages [8] over a grid with collocated pressure and flow nodes.

The grid points $0,1,3,\ldots,2N+1$ are associated with pressure variables $\psi_0(\tau),\psi_1(\tau),\psi_3(\tau),\ldots,\psi_{2N+1}(\tau)$ while the points $0,2,4,\ldots 2N,2N+1$ are associated with the flow variables $q_0(\tau),q_2(\tau),q_4(\tau),\ldots q_{2N}(\tau),q_{2N+1}(\tau)$. The spatial distribution of pressure and flow along the transmission line is now approximated by the ansatz

$$\psi(\xi,\tau)=\sum_{i=0,1,3,\ldots}^{\ldots,2N+1}\psi_i(\tau)\,w\psi_i(\xi) \qquad q(\xi,\tau)=\sum_{i=0,2,4,\ldots}^{\ldots,2N,2N+1}q_i(\tau)\,wq_i(\xi) \quad (12)$$

with weighting functions according to Fig. 1. This ansatz is substitued into the equation system (10, 11). As the friction model represented by the dimensionless friction operator f is assumed to be linear, the friction term can be expanded by

$$f(q(\xi,\tau))=\sum_{i=0,2,4,\ldots}^{\ldots,2N,2N+1}f(q_i(\tau))\,wq_i(\xi). \quad (13)$$

After substituting the ansatz (12) into the equations (10, 11) and applying the expansion (13), the left-hand side of the continuity equation is abbreviated by C and the left-hand side of the momentum equation by M in the following sub-section.

3.3 Galerkin method

A Galerkin procedure is now applied to the continuity equation (C) and the momentum balance equation (M). This gives the equations

$$e_1 = \int_0^1 C \cdot w\psi_1 d\xi = 0, \quad e_3 = \int_0^1 C \cdot w\psi_3 d\xi = 0, \quad \ldots, \quad e_{2N+1} = \int_0^1 C \cdot w\psi_{2N+1} d\xi = 0$$

$$e_2 = \int_0^1 M \cdot wq_0 d\xi = 0, \quad e_4 = \int_0^1 M \cdot wq_2 d\xi = 0, \quad \ldots, \quad e_{2N+2} = \int_0^1 M \cdot wq_{2N} d\xi = 0$$

which are derived symbolically in the computer algebra system Maple 11. The equation errors are summed up in the vector

$$\begin{bmatrix} e_1 \\ e_2 \\ \vdots \\ e_{2N+2} \end{bmatrix} = \mathbf{e}\left(\psi_0, \dot{\psi}_0, q_0, \dot{q}_0, \psi_1, \dot{\psi}_1, q_2, \dot{q}_2, \psi_3, \dot{\psi}_3, \ldots\ldots, \psi_{2N-1}, \dot{\psi}_{2N-1}, q_{2N}, \dot{q}_{2N}, \psi_{2N+1}, \dot{\psi}_{2N+1}, q_{2N+1}, \dot{q}_{2N+1}\right)$$

which is a function of all the pressure and flow-rate functions at the grid points. The pressure $\psi_0(\tau)$ and the flow-rate $q_{2N+1}(\tau)$ are prescribed as boundary conditions.

4 Discretization in time and the treatment of viscous fricition terms

The pressure and flow rate functions are now represented by N_τ values on an equidistant time grid $\tau_j = 2\pi\frac{j}{N_\tau}, \quad j = 0,1,2,\ldots N_\tau - 1$. With the notation

$$\boldsymbol{\psi}_i = \begin{bmatrix} \psi_i(\tau_0) \\ \psi_i(\tau_1) \\ \vdots \\ \psi_i(\tau_{N_\tau-1}) \end{bmatrix}, \quad i = 0,1,3,\ldots 2N+1 \qquad \mathbf{q}_i = \begin{bmatrix} q_i(\tau_0) \\ q_i(\tau_1) \\ \vdots \\ q_i(\tau_{N_\tau-1}) \end{bmatrix}, \quad i = 0,2,4,\ldots 2N, 2N+1$$

the $N_\tau \cdot (2N+2)$ scalar unknowns are grouped in vectors representing the pressures and flow-rates at the spatial grid points over one period in time from 0 to 2π. Simple central differences are used to approximate the time derivatives. With the assumption of periodicity these derivatives are

$$\dot{\boldsymbol{\psi}}_i = \frac{N_\tau}{2\pi}\begin{bmatrix} \psi_i(\tau_{N_\tau-1}) - \psi_i(\tau_1) \\ \psi_i(\tau_2) - \psi(\tau_0) \\ \vdots \\ \psi_i(\tau_0) - \psi_i(\tau_{N_\tau-2}) \end{bmatrix}, \quad i = 0,1,3,\ldots 2N+1$$

$$\dot{\mathbf{q}}_i = \begin{bmatrix} q_i(\tau_{N_\tau-1}) - q_i(\tau_1) \\ q_i(\tau_2) - q(\tau_0) \\ \vdots \\ q_i(\tau_0) - q_i(\tau_{N_\tau-2}) \end{bmatrix}, \quad i = 0,2,4,\ldots 2N, 2N+1.$$

The friction operator is defined in the frequency domain by the transfer function in eq. (8). As this is a transcendental transfer function, it cannot be directly mapped to a discrete-time state-space counterpart with a low dimension comparable to the approximation of the differentiation with respect to time by the centered difference scheme. The solution applied in this paper is an approximation of the friction operator by a least-squares optimization in the frequency domain. The friction operator is approximated by the ansatz

$$\mathbf{f} = \begin{bmatrix} f(\tau_0) \\ f(\tau_1) \\ \vdots \\ f(\tau_{N_\tau-1}) \end{bmatrix} = a_{-N_f} \begin{bmatrix} q\left(\tau_{N_\tau-N_f}\right) \\ q\left(\tau_{N_\tau-N_f+1}\right) \\ \vdots \\ \vdots \\ \vdots \\ q\left(\tau_{N_\tau-N_f-1}\right) \end{bmatrix} + \cdots$$

$$+ a_{-1} \begin{bmatrix} q(\tau_{N_\tau-1}) \\ q(\tau_0) \\ q(\tau_1) \\ \vdots \\ q(\tau_{N_\tau-3}) \\ q(\tau_{N_\tau-2}) \end{bmatrix} + a_0 \begin{bmatrix} q(\tau_0) \\ q(\tau_1) \\ q(\tau_2) \\ \vdots \\ q(\tau_{N_\tau-2}) \\ q(\tau_{N_\tau-1}) \end{bmatrix} + a_1 \begin{bmatrix} q(\tau_1) \\ q(\tau_2) \\ q(\tau_3) \\ \vdots \\ q(\tau_{N_\tau-1}) \\ q(\tau_0) \end{bmatrix} + \cdots + a_{N_f} \begin{bmatrix} q\left(\tau_{N_f}\right) \\ q\left(\tau_{N_f+1}\right) \\ \vdots \\ \vdots \\ \vdots \\ q\left(\tau_{N_f-1}\right) \end{bmatrix} \tag{14}$$

with the coefficients a_i computed from a least squares fit of the frequency domain representation of (14) and the transcendental transfer function in (8). The friction model size N_f has to be constrained because a high number of terms in the friction model results in a dense Jacobian of the overall nonlinear equation system.

The equations are implemented in MATLAB in an object-oriented way of programming with objects for the transmission line itself and for the boundary conditions. This implementation provides the computation of the vector of equation errors as well as the Jacobian of the overall system. Standard procedures for the solution of nonlinear systems of equations can be applied to solve the resulting large system of equations. For the following example, the number of unknowns and equations is 67584. Clearly, a sparse storage model has to be used for the Jacobian matrix. The numerical treatment of the equations is not the focus of this paper and will be published separately. The solution for the example shown below was computed by an arclength continuation procedure with the excitation amplitude as a continuation parameter. The continuation procedure was started at zero excitation amplitude where a trivial solution is known.

5 An example

symbol	value	unit	description
ρ_0	860	$\frac{\text{kg}}{\text{m}^3}$	mass density of the pure liquid at reference pressure
p_0	10^5	Pa	reference pressure, equals 1 bar, i.e. atmospheric
ν	$40 \cdot 10^{-6}$	$\frac{\text{m}^2}{\text{s}}$	kinematic viscosity of the pure liquid
E_{liq}	$1.6 \cdot 10^9$	Pa	modulus of compressibility of the pure liquid
α	0.02	-	volume fraction of gas vs. liquid at reference pressure
R_s	287	$\frac{\text{J}}{\text{kg}\cdot\text{K}}$	specific gas constant
T	330	K	temperature
R	$5 \cdot 10^{-3}$	m	internal pipe radius
L	6	m	transmission line length
p_s	$10 \cdot 10^5$	Pa	scale pressure
ω_{exc}	$2\pi \cdot 20$	$\frac{\text{rad}}{\text{s}}$	excitation frequency
Q_{exc}	$5 \cdot 10^{-4}$	$\frac{\text{m}^3}{\text{s}}$	excitation amplitude

Table 1: Physical parameters of the benchmark problem.

In the following, a simple example is set up to test the proposed method. The physcial parameters of this benchmark problem are contained in Table 1. A constant pressure equal to the reference pressure p_0 is maintained at the left boundary of a transmission line while a sinusoidal flow-rate is prescribed at the right end:

$$p(x,t)|_{x=0} = p_0, \quad Q(x,t)|_{x=L} = Q_{exc} \sin(\omega_{exc} \cdot t)$$

At a certain pressure level, for instance at $\psi = \psi_0$, the speed of sound for small perturbations can be computed as the square root of the ratio of the effective modulus of compressibility (the inverse slope of the density function) over the mass density:

$$c = \sqrt{\frac{\left(\frac{1}{p_s} \cdot \frac{\partial}{\partial \psi} \tilde{\rho}\left(\psi\right)\Big|_{\psi=\psi_0}\right)^{-1}}{\rho_0 \tilde{\rho}\left(\psi_0\right)}} \tag{15}$$

An interesting operating point occurs when the transmission line length is a quarter of the wave length $\lambda = \frac{2\pi c}{\omega_{exc}}$. In the undamped linear case, a so-called λ-quarter resonance is excited. For weak damping, the λ-quarter frequency computed from $4L = \frac{2\pi c}{\omega_{exc}}$ is near the value with maximum pressure amplitude at the right-hand side of the transmission line where the sinusoidal flow-rate is excited. Fig. 2 shows the mean density and the speed of sound as a function of the pressure for three different values of the air volume ratio α. The example with a pressure level of 1 bar and $\alpha = 0.02$ results in $\rho \approx 843$ kg/m³ and $c \approx 78.4$ m/s. While the density is near the value of 860 kg/m³ for the pure liquid, the speed of sound is far below the value of $\sqrt{1.6 \cdot 10^9/860} \approx 1364$ m/s computed in the absence of gas bubbles. The excitation frequency for a λ-quarter resonator at 1 bar and $\alpha = 0.02$ is $f_{exc} = \frac{c}{4L} \approx 19.6$ Hz for the data provided in Tab. 1.

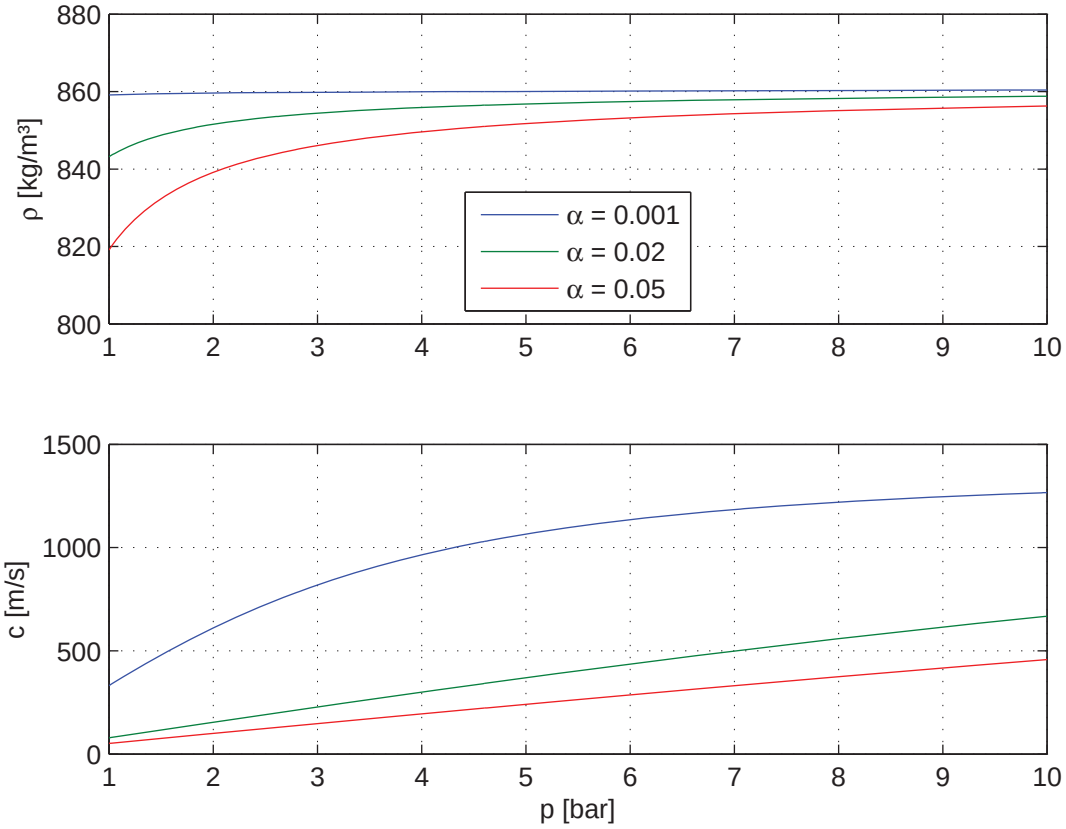

Figure 2: Mean density and speed of sound as a function of pressure.

A periodic solution computed by the proposed method with a spatial grid size of $N = 120$ and a number of $N_\tau = 128$ points in time for an excitation frequency of $f_{exc} = 20$ Hz is depicted in Fig. 3.

6 Summary and conclusding remarks

The equations for the wave propagation in a fluid filled transmission line have been solved for a special material law which describes the behaviour of a mixture of a liquid and a gas. The liquid is weakly compressible with a constant bulk modulus of compressibility and the gas is assumed to be evenly distributed throughout the liquid in the form of small bubbles with an isothermal state change without any dynamics in the material law. Especially the process of air release and back-solution is not modelled. The combined behaviour of the liquid and gas fractions has been cast into a material law giving the mean mass density of the liquid and gas mixture as a function of the hydrostatic pressure. This algebraic equation has been substituted into the equations derived form first principles, i. e. the conservation equations for mass and momentum in axial direction. The viscous friction was modelled using a transfer function known as the frequency-dependent friction model for transient, laminar pipe flow. After a discretization in space using a Galerkin approach on a staggered grid and a discretization in time by a simple point-collocation scheme with centered differences for the time derivatives, a large equation system was solved for the periodic answer to the sinusoidal flow-rate excitation. The result given in Fig. 3 clearly shows the strong impact

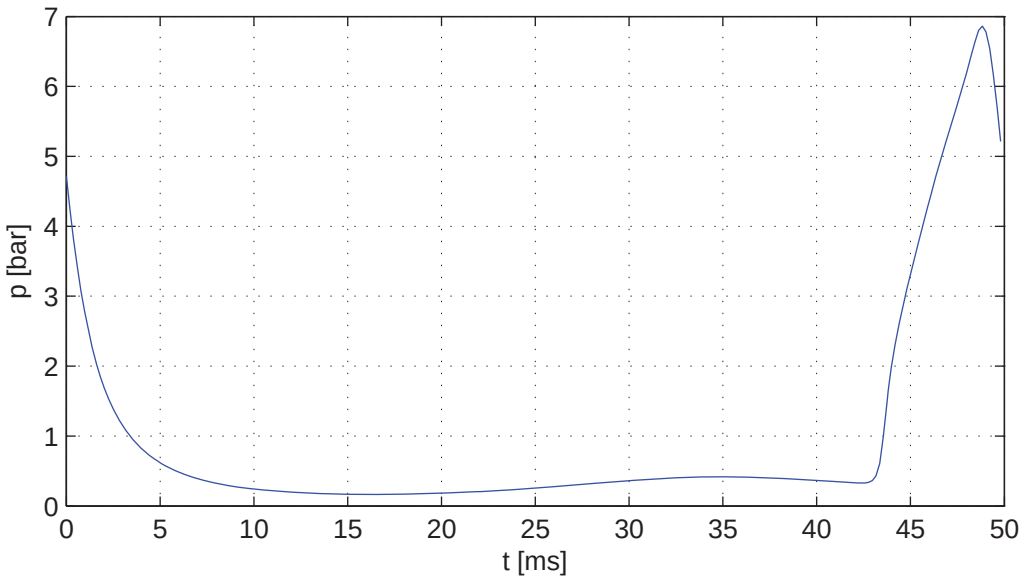

Figure 3: Periodic solution for the pressure at the flow-rate excitation point (right boundary).

of nonlinear effects on the solution behaviour. While the system without gas bubbles has an almost constant speed of sound at least for moderate pressure variations, the solution of the nonlinear system is far from an harmonic response. A broad region of very low pressure is due to the influence of the highly compressible gas fraction which provides of a very large compliance of the fluid column within the transmission line at low pressure values. However, the incoming wave hitting the flow-rate boundary condition generates a high pressure peak due to the progressive stiffness behaviour. All in all, the proposed approach is capable of reproducing some phenomena observed in low pressure lines of fluid power systems. The experimental verification – probably together with some amendments to the model – will be published by the author in the near future.

7 References

[1] A.F. D'Souza and R. Oldenburger. Dynamic response of fluid lines. *Trans. ASME, J. Basic Engng*, 86:589–598, 1964.

[2] F. Franzoni, M. Milani, and L. Montorsi. Deveoping and tailoring a CFD code for multiphase multicomponents flows. In A. Sobczyk, editor, *5th FPNI PhD Symposium*, pages 348–364. FPNI - Fluid Power Net International, 2008.

[3] R. E. Goodson and R. G. Leonard. A survey of modeling techniques for fluid transients. *Transactions of the ASME - Journal of Basic Engineering*, 94(2):474–482, 1972.

[4] A.S. Iberall. Attenuation of oscillatory pressures in instrument lines. *J. Res. Natn. Bur. Std., USA*, 45:85–108, 1950.

[5] N. E. Joukowsky. Über den hydraulischen Stoß in Wasserleitungsrohren. *Memoires de 1 Academie Imperiale des Sciences de St. Petersbourg*, 8, 1900.

[6] B. Manhartsgruber, G. Mikota, and R. Scheidl. Modeling of a switching control hydraulic system. *Mathematical and Computer Modelling of Dynamical Systems*, 11, 2005.

[7] S.V. Patankar. *Numerical heat transfer and fluid flow*. Hemisphere, 1980.

[8] J.-J. Shu, C.R. Burrows, and K.A. Edge. Pressure pulsations in reciprocating pump piping systems, part 1: modelling. *Proc. Instn. Mech. Engrs.*, 211(I):229–237, 1997.

[9] Benjamin E. Wylie and Victor L. Streeter. *Fluid Transients in Systems*. Prentice Hall, 1993.